

# Terahertz laser velocity modulation spectroscopy of ions

Serena K. Stephenson<sup>a</sup>, Richard J. Saykally<sup>b,\*</sup>

<sup>a</sup> ARS-USDA, Albany, CA, USA

<sup>b</sup> Chemistry Department, D31 Hildebrand Hall, University of California-Berkeley, Berkeley, 94720 CA, USA

Received 13 October 2004; in revised form 10 January 2005

Available online 17 February 2005

## Abstract

Velocity modulation spectroscopy has been investigated in the terahertz region, employing pure rotational transitions of  $\text{ArH}^+$  and rotation-tunneling transitions of  $\text{H}_3\text{O}^+$  to study the competition between pressure broadening and Doppler broadening on the lineshapes, neutral suppression, and modulation efficiency. Velocity modulation is demonstrated to be effective to frequencies as low as  $60\text{ cm}^{-1}$ , yielding S/N values for  $\text{ArH}^+$  (770/1) that surpass published terahertz FM results by an order of magnitude.

© 2005 Elsevier Inc. All rights reserved.

**Keywords:** Terahertz; Spectroscopy; Velocity modulation; Ions; Rotational; Vibrational

## 1. Introduction

There is current interest in performing high-resolution ion-selective spectroscopy in the terahertz region ( $30\text{--}300\text{ cm}^{-1}$ ) [1]. Of particular interest is the study of protonated water clusters, since measurements in this low energy region would sample only the lowest intermolecular tunneling splittings, similar to those observed for neutral water clusters [2] vibrations. Tunneling information would provide new insight into hydrogen bond rearrangement dynamics in these clusters. It has been shown that one of the critical aspects of studying ions in the terahertz region is to have a method of distinguishing signals due to ionic and neutral species [1], which is the major strength of velocity modulation spectroscopy.

Velocity modulation spectroscopy has been successfully applied for the study of many positive and negative ions across the spectrum from the mid-IR to the UV [3], and most recently, in the millimeter wave region [4,5].

Because both Doppler shifts and Doppler linewidths are proportional to the transition frequency, it follows that the ratio of the two (the modulation depth) is independent of frequency [6] when the dominant line broadening mechanism is Doppler (inhomogeneous) broadening. This condition is satisfied throughout the region traditionally employed for velocity modulation, wherein the vibration-rotation-tunneling spectrum of  $\text{H}_3\text{O}^+$  at  $\sim 373\text{ cm}^{-1}$  constitutes the lowest frequency velocity modulation measurement [7], and the  $\sim 17000\text{ cm}^{-1}$  rovibronic transitions of  $\text{H}_2\text{O}^+$  the highest [8]. In light of the recent extension of velocity modulation to  $<500\text{ GHz}$  ( $<16.6\text{ cm}^{-1}$ ) and the present work extending it from  $60$  to  $100\text{ cm}^{-1}$ , the assumption that one must be strictly in the Doppler limit for velocity modulation to be effective must be reassessed. Factors such as buffer gas composition, operating pressure, temperature, and cell dimensions all influence the extension velocity modulation below its traditional frequency range. In practice, there seems to be no rigorous lower limit to the frequency at which velocity modulation experiments can be performed.

Velocity modulation relies on the condition that the Doppler shift induced by the electric field in the plasma

\* Corresponding author. Fax: +1 510 642 8369.

E-mail address: [saykally@uclink4.berkeley.edu](mailto:saykally@uclink4.berkeley.edu) (R.J. Saykally).

is comparable to the linewidth of the peak [9]. This condition holds in spectral regions wherein Doppler broadening is the primary source of the peak width. However, in the terahertz region, collisional broadening becomes significant, and does not scale rapidly with frequency, but instead, the width of a transition increases with operating pressure. However, since  $E/P$  is approximately constant for a given buffer gas, as pressure increases so does the plasma electric field. This subsequently increases Doppler shift at higher pressures. The electric field is also dependent on the polarizability of the buffer gas, implying that adjustment of the buffer gas mixture can cause a significant change in the Doppler shift of a transition. This results in complicated behavior, generally ignored at high frequencies, to the modulation index, defined as the (Doppler shift)/(line width) [9]. If the modulation index decreases, as would be the case if the Doppler shift does not increase as much as the does total linewidth with increasing pressure, the result is a loss of sensitivity. The terahertz region is therefore one in which small changes in experimental conditions, affecting either the shift or the width of a spectral transition, can spell the difference between success or failure in observing an ion spectrum. This same holds true for the sub-millimeter wave velocity modulation experiment [4,5]. Due to the technical difficulties attending the velocity modulation experiment at these low frequencies, only a few such studies have been done. The main obstacles encountered are the production of tunable terahertz radiation with high enough powers and sufficient spectral coverage to perform useful direct absorption spectroscopy experiments [10,11], generating stable glow discharges at low enough pressures to minimize the collisional broadening while maintaining sufficient ion densities, and removing background on the detector caused by the presence of the AC electric field in the plasma. The focus of this paper is the minimization of these factors in the terahertz region, but in the conclusion section we present a brief comparison between this and the sub-millimeter VM experiment.

The first of the molecular ions studied here,  $\text{ArH}^+$ , has pure rotational transitions throughout the terahertz region. This ion has been well characterized in frequency-modulated experiments involving DC plasmas, and therefore it is convenient to use as a test molecule, since production conditions are known, and exact rotational transition frequencies are available in the literature. The second ion,  $\text{H}_3\text{O}^+$ , is of primary interest as the precursor for protonated water clusters such as  $\text{H}_5\text{O}_2^+$  and  $\text{H}_7\text{O}_3^+$ . The band origin for the pure inversion motion of the hydronium ion is near  $55\text{ cm}^{-1}$ , so there are many possible transitions below  $100\text{ cm}^{-1}$ . Unfortunately, many of these transitions have never actually been observed, so their frequencies had to be calculated by combination differences.

## 2. Theory

The Doppler shift and the Doppler width are the essential parameters of the velocity modulation experiment. The modulation index, also called the modulation depth, is the ratio of the peak shift to width and must approach unity in order for a transition to be completely modulated. The (first order) Doppler width of a transition is proportional to the randomized translational motion of the species whereas the directional (viz. axial) portion of the ion drift velocity is manifested in a corresponding Doppler shift. The zero-field Doppler width is given by

$$\Delta\nu_D \cong 3.581 \times 10^{-7} v_0 \left[ \frac{T_{\text{eff}} (\text{Kelvin})}{m (\text{a.m.u.})} \right]^{1/2}, \quad (1)$$

where  $v_0$  is the transition frequency,  $T_{\text{eff}}$  is the “effective ion translational temperature” and  $m$  is the ion mass [6,12]. The Doppler shift is given by

$$\delta\nu = v_0 \left( \frac{v_{\text{da}}}{c} \right), \quad (2)$$

where  $\delta\nu$  is the Doppler shift,  $v_0$  is the center frequency of the transition,  $c$  is the speed of light (cm/s), and  $v_{\text{da}}$  is the axial drift velocity (cm/s) of the ion in the plasma [6,12]. The axial drift velocity itself contains much information. It is defined as

$$v_{\text{da}} = K \cdot E, \quad (3)$$

with  $K$  being the ion mobility ( $\text{cm}^2/\text{V s}$ ) and it  $E$  being the axial electric field (V/cm) [6,12]. Most ion mobility values listed in the literature are in the form of the reduced mobility ( $K_0$ ), which allows values to be compared across experiments. The mobility and the reduced mobility are related by

$$K = K_0 \left[ \frac{760}{P (\text{Torr})} \right] \left[ \frac{T_{\text{neut}} (\text{Kelvin})}{273.16} \right], \quad (4)$$

where  $P$  is the total pressure and  $T_{\text{neut}}$  is the translational temperature of the neutral atoms or molecules within the plasma [6,12]. The typical method of calculating the reduced mobility for a system is to use the Langevin formalism

$$K_0 = \frac{13.876}{\sqrt{\alpha \cdot \mu}}, \quad (5)$$

where  $\alpha (\text{\AA}^3)$  is the dipolar-polarizability of the neutral collision partner, and  $\mu$  (a.m.u.) is the reduced mass of the ion–neutral collision pair. This includes only the induced dipole interaction and neglects higher order terms. One note about using mobilities in the calculation of the Doppler shift is that experiments often employ a mixture of neutral gases, with different polarizabilities and reduced masses, comprising the bulk of the buffer gas. In this case, a type of weighted average of the mobilities of the individual constituents can be used following Blanc’s Law [13]

$$\frac{1}{K_{\text{mix}}} = \frac{\chi_1}{K_1} + \frac{\chi_2}{K_2} + \dots, \quad (6)$$

where  $\chi$  is the mole fraction of a given component of the mixture.

Both the axial and radial electric fields in the glow discharge plasma are approximately proportional to pressure, with  $E/P$  being a characteristic property of a given buffer gas. Moreover,  $E$  scales with the density of accessible states of a gas, since it must be sufficient to maintain the charge density required for a specified current (current = charge density  $\times$  mobility). This implies that both the directed and randomized ion velocities, and therefore the Doppler shift and width, will increase as  $E$  increases, albeit not at exactly the same rate. Since the pressure broadening linewidth is also proportional to pressure, the modulation index will depend on the specific pressure dependences of all three of these properties.

The remaining information needed for a theory of velocity modulation in the terahertz region, are the equations used to describe pressure broadening. There are two useful ways to think about the pressure broadened linewidth. The first uses the mean time between collisions ( $\tau$ ) and the second, is to use the temperature-dependent collisional rate constant. The peak due to pressure broadening ( $\Delta\nu_p$ ) is then given by

$$\Delta\nu_p \text{ (HWHM)} = \frac{1}{2\pi\tau}. \quad (7)$$

Here,  $\tau$  is the time between reactive or “strong” collisions. The definition of a strong collision is one that results in a significant perturbation of the rotational phase of the ion, or a reaction between the ion and a neutral collision partner. There is some latitude in the definition of a strong collision in that the extent of the perturbation is not specified. Eq. (8) uses the temperature-dependent rate constant, rather than the mean time between collisions, to calculate the width:

$$\Delta\nu_p \text{ (HWHM)} = \frac{k(T)}{2\pi k T_{\text{neut}}} \cdot P. \quad (8)$$

Here,  $k(T)$  is the temperature-dependent rate constant,  $P$  is the total pressure in the cell (Torr),  $k$  is the Boltzmann constant, and  $T_{\text{neut}}$  is the neutral temperature of the plasma (K).

Since the temperature dependent rate constants for plasma conditions are difficult to calculate empirically, the temperature-independent rate constant from Langevin capture theory, as described by Pearson et al. [14], can be substituted in Eq. (8) as a method of calculating the expected width of a transition. Langevin theory gives the temperature-independent rate constant as

$$k_L = 2\pi q \sqrt{\alpha/\mu}, \quad (9)$$

where  $q$  (esu) is the electronic charge,  $\alpha$  (cm<sup>3</sup>) is the polarizability of the neutral buffer gas molecule, and  $\mu$

(g) is the reduced mass of the ion–neutral collision pair. This is the equation that describes reactive collisions between ions and non-polar neutrals [15,16]. Making the assumption that every collision which obeys the criteria for capture by this theory is either reactive, as the theory provides, or strongly perturbs the rotational phase of the ion, this Langevin rate constant can be substituted for  $1/\tau$  by multiplying  $k_L$  by the gas density.

In considering all of the variables that contribute to the lineshape of a velocity modulation transition, it is helpful to see how each of them changes the Doppler shift, Doppler width, and the pressure-broadened width. This is shown in Table 1. The variables over which there is the most experimental control are the neutral temperature ( $T_{\text{neut}}$ ) and the pressure ( $P$ ). Variation in  $\mu$  is the reduced mass of the ion–neutral collision pair, and  $\alpha$  is the polarizability of the neutral, can be achieved by changing the buffer gas in the plasma. However, there is a compromise between buffer gases that minimize the reduced mass and polarizability, but at the same time do not significantly alter the plasma chemistry for production of the ion of interest. Different buffer gases effect different electric field magnitudes (both axial and radial) as the pressure in the discharge changes, and this complicates the dependence of the Doppler shift,  $\delta\nu$ , of a transition, but generally, the lower the pressure is, the larger the resulting shift. The table shows, the shift  $\delta\nu$  is inversely proportional to  $\sqrt{\alpha}$  while  $\Delta\nu_p$  is proportional to it. In other words, the larger the polarizability of the plasma buffer gas, the smaller the shift and the bigger the pressure broadened width. This implies that at low frequencies, the optimum buffer gas is one with a small polarizability. In addition, there is a balance for the ideal pressure and cell diameter to use in the terahertz region. Looking at Table 1, it is evident, by reasoning involving the Doppler shift and pressure broadened width, that the lower the pressure is, the better suited the system is low frequency velocity modulation. This was observed to be somewhat important in our terahertz studies, with optimal pressures being near 1350–1600 mTorr, and absolutely vital in the sub-millimeter experiments where pressures near 50 mTorr were ideal. However, if the pressure is too low, the glow discharge plasma becomes unstable; the concentration of ions diminishes, and the electric field may be too small to induce a sufficient Doppler shift in the ion.

To illustrate how the Doppler shift, and the two contributions to the width compare over a range of frequencies, Fig. 1 shows a series of four plots of calculations for  $\text{ArH}^+$  in two different buffer gases and using two different electric field values. Simplifying assumptions have been made here. The first is that there is no mixing of buffer gases (i.e., the  $\text{ArH}^+$  ion is in the midst of a plasma comprised entirely of either Ar or He). Second, all of these plots were calculated for  $T_{\text{neut}} = 700$  K, and a total pressure of 1.3 Torr. Third, the electric field values used

Table 1

This table shows how all of the different variables affect the critical peak shifts and Doppler widths

Linearly proportional to...								
$\delta\nu$	$\nu_0$	$1/P$	$T_{\text{neut}}$	$1/\sqrt{\alpha}$	$1/\sqrt{\mu}$	—	$E$	—
$\Delta\nu_d$	$\nu_0$	—	$\sqrt{T_{\text{eff}}}$	—	—	$1/\sqrt{m}$	$E^a$	—
$\Delta\nu_p$	—	$P$	$1/T_{\text{neut}}$	$\sqrt{\alpha}$	$1/\sqrt{\mu}$	—	—	$q$

The variables are as follows:  $\nu_0$  is the transition frequency,  $P$  is the pressure (Torr),  $T$  is the temperature (K),  $\alpha$  is the polarizability of the neutral ( $\text{cm}^3$ ),  $\mu$  is the reduced mass of the ion–neutral collision pair (g),  $m$  is the mass of the ion (a.m.u.),  $E$  is the electric field (V/cm), and  $q$  is the ionic charge (esu).

<sup>a</sup> This may not be linearly proportional as the relation comes from the  $E$  dependence of  $T_{\text{eff}}$ .

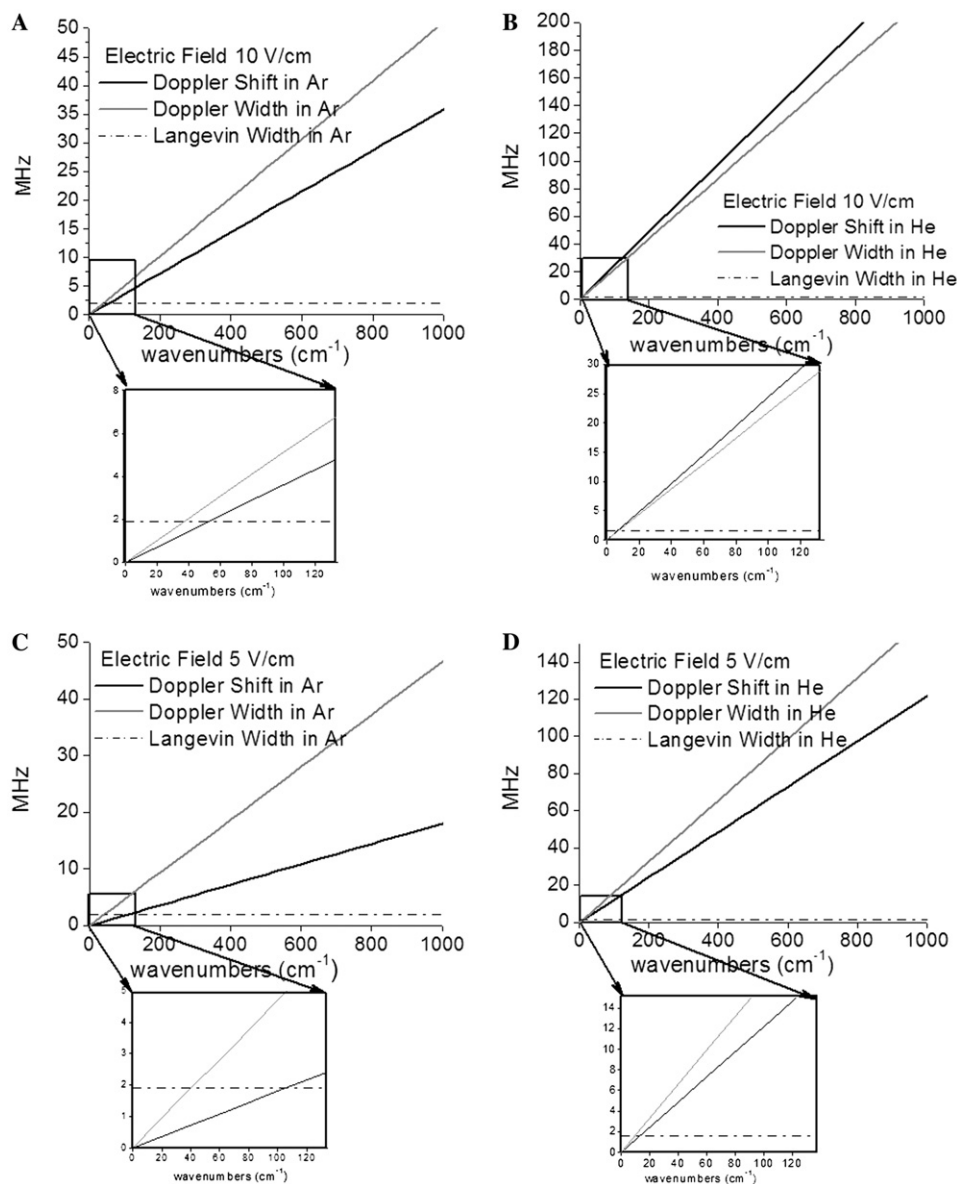


Fig. 1. Calculated shifts and widths of  $\text{ArH}^+$  over the range of 0–1000  $\text{cm}^{-1}$ . The first two are for a 10 V/cm field with (A) Ar and (B) He. The second two are for a 5 V/cm field with (C) Ar and (D) He.

are two values in the range typically cited as to axial electric field values in a glow discharge. The goal is to get a qualitative idea of the frequency cutoff for making the Doppler limit approximation. Figs. 1A and B show

these calculations for 10 V/cm in Ar and He, respectively. Figs. 1C and D show both of these situations for a 5 V/cm electric field. The insets on each of these plots expand on the frequency region below 130  $\text{cm}^{-1}$

where the Langevin width becomes greater than either the Doppler width or the Doppler shift.

Comparing the modulation depths of these four examples in the higher frequency regions shows that it is actually above 1 only for case (b). In Ar (5 V/cm field), the modulation depth is 0.4, but in both Ar (10 V/cm) and He (5 V/cm), it is only 0.7. In the case of He with a 10 V/cm field, the modulation depth is 1.1. It is only in this extreme case that an  $\text{ArH}^+$  transition at  $100\text{ cm}^{-1}$  is sufficiently in the Doppler limit so that contributions from the Langevin width can be neglected. In this case, the cutoff is at  $\sim 65\text{ cm}^{-1}$ . In the case of He with a 5 V/cm field, this cutoff falls at  $\sim 100\text{ cm}^{-1}$ , and both the examples with Ar yield cutoffs above  $\sim 400\text{ cm}^{-1}$ . The frequency “cutoffs” here are not limits that VM is unable to transcend, but rather the limits for which the signals are fully modulated and have widths determined by Doppler broadening alone. With all of this information taken into account, it is apparent that velocity modulation can function as a sensitive ion selective spectroscopic technique in the terahertz region, and with the careful adjustment the experimental parameters and plasma conditions, it works even in the sub-millimeter wave region.

The plots in Fig. 1 are solely for examining the influence of the frequency of a transition on the modulation depth. There is, however, another critical factor in the modulation depth, and that is the dependence of the electric field on the specific buffer gas. Since  $E/P$  is constant for a given buffer gas, the electric field increases with the pressure. Also, the electric field will increase with the density of states of the buffer gas, due to inelastic collisions. In general between Ar and He at the same pressures in a discharge, Ar will have the higher field, resulting in a larger modulation index. However, since the Doppler shift is also inversely proportional to the polarizability (Table 1) of the buffer gas, and because of the cooling effect of He, the contribution of the increased density of states in Ar could be mitigated, and under some conditions He could actually generate a larger modulation index. This possibility is supported by Fig. 4, and discussed further in that context.

### 3. Background

All of the previous terahertz velocity modulation studies have been performed by Takagi's group in Japan [17,18]. They have studied the pure rotational spectra of noble gas-hydrogen complexes from  $\text{HeH}^+$ ,  $\text{NeH}^+$ ,  $\text{ArD}^+$ , and  $\text{KrH}^+$  using a tunable terahertz laser system designed by Evenson et al. [11]. The “TuFIR” system used in their work generates tunable light throughout the terahertz region by mixing two  $\text{CO}_2$  laser beams and tunable microwave radiation in a MIM diode (metal-insulator-metal) [17,19]. Velocity modulation was only used in the study of the lighter species,  $\text{HeH}^+$

and  $\text{NeH}^+$  [17,18], and it was reportedly not effective for  $\text{KrH}^+$  [19]. The argument given by Odashima et al. [20] is that the higher mass of  $\text{KrH}^+$  makes it unobservable by velocity modulation, but this is questionable since both the Doppler shift and the linewidth track with mass so this should result in no net change of the modulation index. Nevertheless, they used source modulation, rather than velocity modulation, to study  $\text{ArD}^+$  and  $\text{KrH}^+$ .

The sample cell used in the studies by Matsushima et al. [18] was a liquid nitrogen cooled Pyrex tube, which was 1.4 m long with an inner diameter of 1.6 cm. The AC discharge was run at 1.2 kHz with a current density of  $\sim 180\text{ mA/cm}^2$ . The  $J = 1 \leftarrow 0$  transition of  $\text{HeH}^+$ , located at 2010.18387 GHz, was observed using a scan rate of 1.66 MHz/s and a 0.3 s time constant on the lock-in amplifier [18]. This result was then averaged over six scans yielding a peak with S/N of  $\sim 15/1$ . The same scan rate, time constant, and averaging scheme were used for  $\text{NeH}^+$  as well as its isotopes. The  $J = 4 \leftarrow 3$  transition of  $^{20}\text{NeH}^+$ , which is located at 4137.6729 GHz, was observed with a S/N of  $\sim 200/1$  [17]. This transition actually occurs at about  $140\text{ cm}^{-1}$ , slightly above the region for which there is the most concern about the role of pressure broadening in hindering the velocity modulation technique. In the next section, these results will be compared against those achieved with the Berkeley Terahertz Spectrometer, adapted for velocity modulation.

The case of  $\text{ArD}^+$  is interesting in that both velocity and source modulation techniques were used [21].  $\text{HeH}^+$  and  $\text{NeH}^+$  can also be observed with both techniques, but only velocity modulation was used. It is claimed that intensities for  $\text{ArD}^+$  were the same for both schemes [21], indicating that the modulation depth from velocity modulation is the same as that from source modulation. There is no specification as to which rotational line of  $\text{ArD}^+$  was being studied when this was observed [21]. In their study on the rotational spectrum of  $\text{ArD}^+$ , source modulation, rather than velocity modulation, was used. Unfortunately, there are no velocity modulated  $\text{ArH}^+$  transitions published in the literature to which comparisons can be made, so the frequency modulated  $J = 6 \leftarrow 5$  peak published by Brown et al. [22] will be used instead.

### 4. Experimental

Two molecular ions have been observed below  $\sim 105\text{ cm}^{-1}$  using the VM setup shown in Fig. 2 with the Berkeley Terahertz Spectrometer as the light source. The Berkeley Terahertz Spectrometer has been previously described in detail [10]. The setup for these experiments used a water-cooled discharge cell which was  $\sim 1\text{ m}$  long with inner diameters ranging from 1 to 3 cm and a discharge frequency of  $\sim 25\text{--}30\text{ kHz}$  with

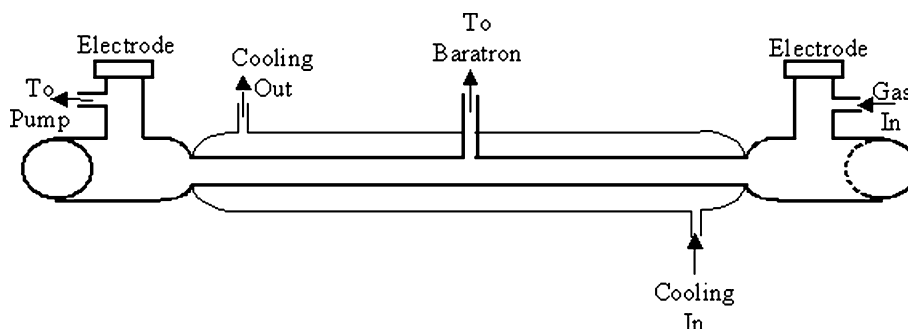


Fig. 2. A diagram of the AC glow discharge cell showing the electrode location, the cooling jacket, the gas inlet and outlet and the connection to the Baratron pressure gauge.

currents between 500 and 600 mA. A schematic of the cell is displayed in Fig. 2. The end pieces have polyethylene windows at Brewster angles of  $34.5^\circ$  (tolerance  $\pm 1^\circ$ ), and there is an off-axis electrode at each end. One of these electrodes is connected to ground via a current monitor, and the other is the “hot” electrode, which switches between positive and negative high voltage as powered by a Plasmaloc 2 power supply. This Plasmaloc provides a high voltage AC current at frequencies between 25 and 125 kHz. This voltage is stepped up by a ENI RS-816T transformer before passing through a 1 k $\Omega$  ballast resistor and being applied to the hot electrode. The best results were found with cells of inner diameters of 1.5 or 2 cm. It was found that glass tube of the velocity modulation cell actually acted as a waveguide for the terahertz light. As long as the light was focused into the start of the cell there was no loss of intensity at the detector. In most cases, transitions were measured with a single scan (i.e., no averaging of multiple traces) at a scan rate of  $\sim 1$  MHz/s and a time constant of  $\sim 1.25$  s.

## 5. Results

### 5.1. $\text{ArH}^+$

The rotational transitions of  $\text{ArH}^+$  as given by Brown et al. [22] are listed in Table 2. The two transitions studied here are the  $J = 3 \leftarrow 2$  at 1845789.0 MHz ( $61.5 \text{ cm}^{-1}$ ) and  $J = 5 \leftarrow 4$  at 3070392.8 MHz

( $102.4 \text{ cm}^{-1}$ ). The conditions, which produced the largest S/N values, were achieved by using the 1.5 cm inner diameter cell with water cooling. A 30 kHz AC voltage, applied across the electrodes, produced a current of  $\sim 550$  mA. The pressure inside the cell was measured by a Baratron manometer, and the gas mixture consisted of  $\sim 4$ –6 mTorr  $\text{H}_2$ ,  $\sim 600$ –800 mTorr Ar with the balance He, creating a total pressure of between  $\sim 1350$  and 1600 mTorr. Within these limits, the intensities of the observed velocity modulation peaks were constant. That is, regardless of whether there was 4 mTorr  $\text{H}_2$  and 800 mTorr Ar, with a total pressure of 1500 or 6 mTorr  $\text{H}_2$  and 600 mTorr Ar, with a total pressure of 1350 mTorr, the signal to noise ratios of the recorded peaks varied by only 5%.

A comparison of the  $J = 3 \leftarrow 2$  to the  $J = 5 \leftarrow 4$  transition is shown in Fig. 3 including peaks resulting from both 1f and 2f lock-in demodulation of the velocity modulated signal. Fig. 3A shows a single scan of the  $J = 5 \leftarrow 4$  transition, which was scanned at a rate of 1 MHz/s with a total pressure in the VM cell of 1346 mTorr, yielding a 1f signal with S/N of  $\sim 770/1$ . The ratio of the intensity of the 2f signal to that of the 1f signal is 0.84, indicating that in this situation the transition is modulated to a large enough extent so as not to lose much intensity. However, Fig. 3B shows the 1f and 2f peaks from the  $J = 3 \leftarrow 2$  transition measured under the same conditions. In this case, it was necessary to average multiple scans to generate large enough S/N to fit the line-shape using a least-squares routine. Even then, a S/N of 15/1 was the best that was achieved for  $J = 3 \leftarrow 2$ . The small intensity is probably due a combination of two factors. The first is that, since the plasma is water-cooled, rather than liquid  $\text{N}_2$  cooled, the warm temperature of the plasma puts more of the population in higher rotational levels. The second, and most important contribution to the small intensity is under-modulation of the ion at these low frequencies ( $60 \text{ cm}^{-1}$ ), which is supported by comparing the 1f and 2f signals. The 2f signal is five times larger than that of the 1f signal indicating that the 1f transition is seriously under-modulated (i.e.,  $\delta v / \Delta v_{\text{tot}} \ll 1$ ). It is impossible to calculate

Table 2

The pure rotational transitions for  $^{40}\text{ArH}^+$  as reported by Brown et al. [22]

Transition $J$	Observed frequency (MHz)
$1 \leftarrow 0$	615858.4
$2 \leftarrow 1$	1231271.18
$3 \leftarrow 2$	1845793.67
$4 \leftarrow 3$	2458981.89
$5 \leftarrow 4$	3070392.15
$6 \leftarrow 5$	3679583.52

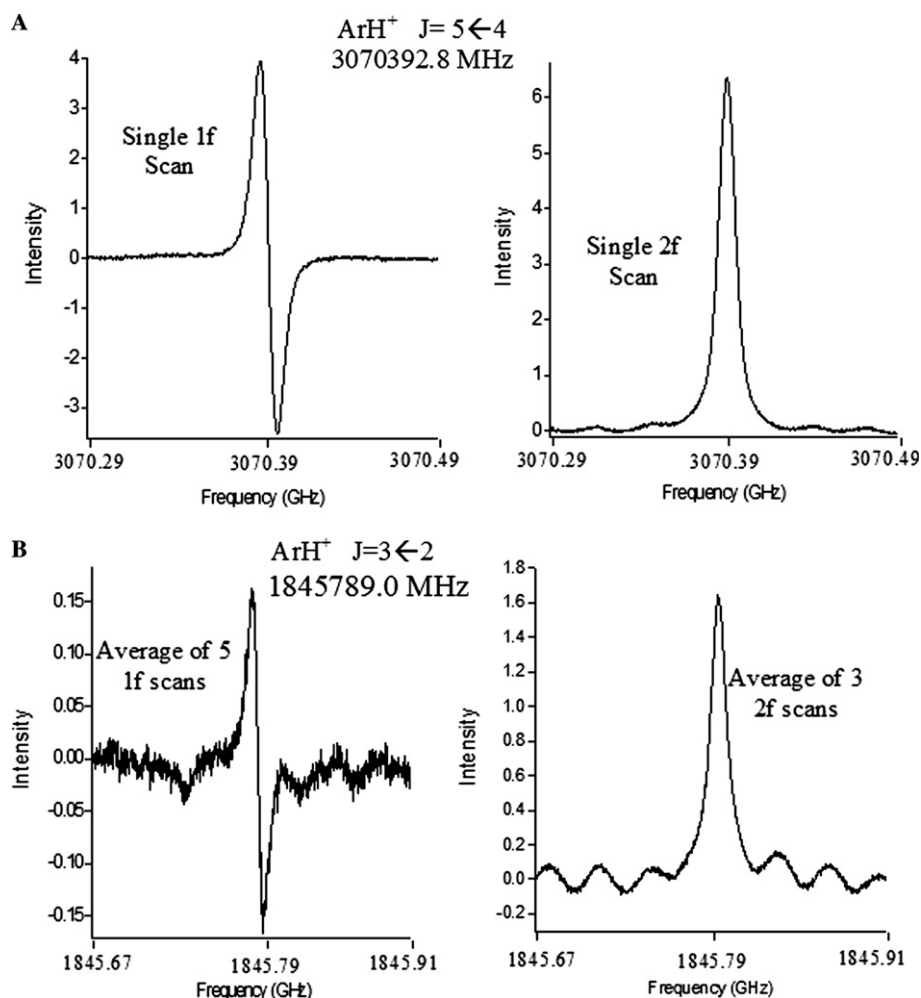


Fig. 3. Scans of two rotational transitions of  $\text{ArH}^+$  observed using terahertz-VM. (A)  $J = 5 \leftarrow 4$  transition at  $\sim 100 \text{ cm}^{-1}$  which has a S/N of 750/1 and similar S/N ratios between the 1f and the 2f peaks. (B)  $J = 3 \leftarrow 2$  near  $60 \text{ cm}^{-1}$  which is much weaker than the peaks shown in (A). Also, the 2f peak is stronger than the peak observed with 1f detection.

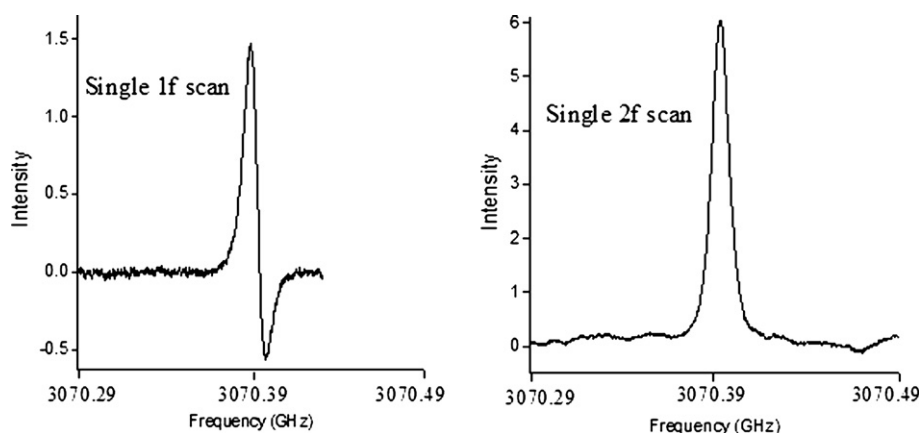


Fig. 4. This is the  $J = 5 \leftarrow 4$  transition of  $\text{ArH}^+$  using 1f and 2f detection of a plasma with no He in the buffer gas. The total pressures are  $\sim 5 \text{ mTorr}$  of  $\text{H}_2$  and  $\sim 800 \text{ mTorr}$  of Ar.

the exact modulation depth for either of these transitions because even when doing a simultaneous fit of the 1f and 2f peaks, the shift and width are highly coupled.

It was found that the presence of He in the buffer gas of the plasma was essential for achieving large signal to noise values. Fig. 4 illustrates this point by showing the  $J = 5 \leftarrow 4$  transition at lower overall pressures with a

gas mixture containing no He. In 1f, the S/N is nearly four times smaller with no He than when 500 mTorr of He is added to the plasma, but the S/N of the 2f signal is only slightly smaller without He, decreasing from 650/1 (with He) to 600/1 (without He). This indicates that, although the chemistry of forming  $\text{ArH}^+$  in the plasma may have something to do with the increased intensity effected by adding helium, this is primarily due to the increase in modulation depth caused by the increasing Doppler shift and decreasing pressure broadened width which arise from adding a buffer gas with such low mass and small polarizability. The smaller mass and polarizability of helium as the buffer gas causes enough of an increase in the mobility of the ion that the effects of the increasing pressure, which would otherwise decrease the modulation depth, are overwhelmed by the increase in the Doppler shift, resulting in an increased modulation depth. The asymmetry shown by this peak at low pressures was reproducible and was likely caused by asymmetry in the AC discharge. The VM experiment in the sub-millimeter region also resulted in an asymmetric peak profile unless careful adjustment of experimental parameters was performed [4,5]. It seems likely that the asymmetry results from the fact that a high pumping speed was maintained in one direction through the cell, resulting in a pressure drop and corresponding asymmetry in the two polarities of the discharge. Overall, the observation of  $\text{ArH}^+$  with large intensities (770/1) at low frequencies is encouraging for the prospect of using terahertz VM to study other ions. It should be noted that the 770/1 S/N ratio for  $\text{ArH}^+$  shown in Fig. 3A represents approximately a factor of 50 increase over that reported for  $\text{HeH}^+$  by Odashima et al. [21], and an about an order of magnitude increase when compared to the S/N of the frequency-modulated  $\text{ArH}^+$  transition reported by Brown et al. [22].

## 5.2. $\text{H}_3\text{O}^+$

The other ion that was used as a test for the feasibility of terahertz velocity modulation is  $\text{H}_3\text{O}^+$ . Initial studies

of this molecule in the terahertz region were made using frequency modulation, as reported by Verhoeve et al. [23], and from the transitions listed by them, there were two transitions calculated to be at an accessible frequency. Both of these are *R*-branch transitions of the pure inversion band. The first is  $J_{\text{ka}} = 6_1^+ \leftarrow 5_1^-$  at 2519039 MHz ( $84.0 \text{ cm}^{-1}$ ) and the other,  $J_{\text{ka}} = 7_5^+ \leftarrow 6_5^-$ , is predicted at 3077879 MHz ( $102.7 \text{ cm}^{-1}$ ). However, of these two transitions, only the  $7_5^+ \leftarrow 6_5^-$  was observed. The other one was too weak due to the large difference between *J* and *K* quantum numbers. The  $7_5^+ \leftarrow 6_5^-$  peak is shown in Fig. 5. It was maximized using the 1.5 cm inner diameter cell with water-cooling. Compared to  $\text{ArH}^+$ ,  $\text{H}_3\text{O}^+$  is extremely sensitive to the gas composition and pressure within the cell. The largest signal was found with 300–340 mTorr of  $\text{H}_2$  bubbled through liquid  $\text{H}_2\text{O}$  and diluted with another 680–750 mTorr of dry  $\text{H}_2$ . The AC discharge conditions were the same as for  $\text{ArH}^+$  except that the scan rate was 0.8 MHz/s. Adding He as a buffer gas to the  $\text{H}_3\text{O}^+$  mixture not only failed to increase the signal, but actually caused it to disappear. This is partially due to the collisional cooling effect of He because the initial state for this particular  $\text{H}_3\text{O}^+$  transition lies at  $\sim 400 \text{ cm}^{-1}$ . However, it could also be the case that He interferes with the production of  $\text{H}_3\text{O}^+$  in the plasma. We also note that the attempt to measure this same transition using the  $\sim 3:1 \text{ H}_2:\text{O}_2$  mixture used by Radunsky yielded no detectable spectra [24]. Fig. 5 shows the 1f and 2f peaks observed by a single scan over the frequency of interest yielding a signal to noise of  $\sim 7/1$ . This is a weak, but unmistakable, signal located at 3077891.8 GHz. A comparison between the 2f and the 1f intensities gives the ratio to be 1.05, indicating that this signal is fairly well modulated, although, as was the case for  $\text{ArH}^+$ , it is impossible to calculate the actual modulation depth.

## 6. Conclusions

A comparison of the terahertz velocity modulation technique, described here, and the sub-millimeter tech-

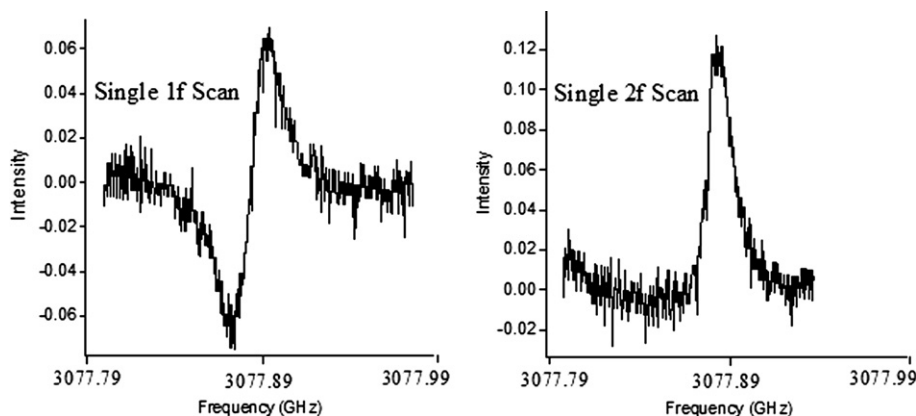


Fig. 5. This is the  $J_{\text{ka}} = 7_5^+ \leftarrow 6_5^-$  pure inversion transition of  $\text{H}_3\text{O}^+$  located at 3077891.8 MHz as observed by velocity modulation.

nique, presented by Savage and Ziurys [5], reveals that the two experiments required different parameters to yield successful velocity modulated spectra. There are three major differences between the experiments. The first is the operating pressure. Sub-mm VM requires pressures that are 30 times lower than those that optimize signals in the terahertz (50 mTorr versus 1500 mTorr). It is because of these low pressures that they are able to avoid modulation index problems due to pressure broadening. The other major difference is the cell diameter, which ranges from 1.5–2 cm to 10 cm, for terahertz and sub-millimeter regions, respectively. This increases (in proportion to the diameter) the lifetime of the ion before destruction by collisions with the wall of the cell, but it decreases (by the square of the diameter) the number density of ions in the plasma. The S/N ratios observed for  $\text{SH}^+$  by Savage et al. are only  $\sim 5/1$  even after the averaging of four scans. In the terahertz system, however, multiple scan averaging was not necessary to yield S/N values of 770/1 for  $\text{ArH}^+$  and 7/1 for  $\text{H}_3\text{O}^+$ .

The observation of  $\text{H}_3\text{O}^+$  reported here is the first made in the terahertz regime using velocity modulation, and the measurements of  $\text{ArH}^+$  show an order of magnitude signal to noise improvement when using terahertz VM as compared to frequency modulation in a DC glow discharge [22]. The demonstrations of velocity modulation in the terahertz region and its recent extension into the millimeter-wave region [4,5] have altered the traditional view of VM as a technique limited to infrared and higher frequencies. There are unique characteristics and challenges to VM at such low frequencies, but they clearly can be transcended. Many interesting ionic systems are now accessible to study at these low frequencies.

## Acknowledgments

This work was supported by the Experimental Physical Chemistry Division of the National Science Foundation.

## References

- [1] E.A. Michael, C.J. Keoshian, S.K. Anderson, R.J. Saykally, *J. Mol. Spectrosc.* 208 (2001) 219.
- [2] F.N. Keutsch, R.J. Saykally, *Proc. Natl. Acad. Sci. USA* 98 (2001) 10533–10540.
- [3] S.K. Stephenson, R.J. Saykally, *Chem. Rev.* (submitted).
- [4] C. Savage, A.J. Apponi, L.M. Ziurys, *Astrophys. J.* 608 (2004) L73–L76.
- [5] C. Savage, L.M. Ziurys, *Rev. Sci. Instr.* (in press).
- [6] C.S. Gudeman, R.J. Saykally, *Ann. Rev. Phys. Chem.* 35 (1984) 387–418.
- [7] D. Liu, T. Oka, *Phys. Rev. Lett.* 54 (1985) 1787–1789.
- [8] P. Murtz, L.R. Zink, K.M. Evenson, J.M. Brown, *J. Chem. Phys.* 109 (1998) 9744–9752.
- [9] J.W. Farley, *J. Chem. Phys.* 95 (1991) 5590–5602.
- [10] G.A. Blake, K.B. Laughlin, R.C. Cohen, K.L. Busarow, D.H. Gwo, C.A. Schmittenmayer, D.W. Steyert, R.J. Saykally, *Rev. Sci. Instrum.* 62 (1991) 1701–1716.
- [11] K.M. Evenson, D.A. Jennings, F.R. Peterson, *Appl. Phys. Lett.* 44 (1984) 576.
- [12] N.N. Haese, F.S. Pan, T. Oka, *Phys. Rev. Lett.* 50 (1983) 1575–1578.
- [13] E.A. Mason, E.W. McDaniel, *Transport Properties of Ions in Gases*, Wiley, New York, 1988.
- [14] J.C. Pearson, L.C. Oesterling, E. Herbst, F.C. De Lucia, *Phys. Rev. Lett.* 75 (1995) 2940–2943.
- [15] P. Langevin, *Ann. Chim. Phys.* 5 (1905) 245.
- [16] G. Gioumoussis, D.P. Stevenson, *J. Chem. Phys.* 129 (1958) 294.
- [17] F. Matsushima, Y. Ohtaki, O. Torige, K. Takagi, *J. Chem. Phys.* 109 (1998) 2242–2245.
- [18] F. Matsushima, T. Oka, K. Takagi, *Phys. Rev. Lett.* 78 (1997) 1664–1666.
- [19] F. Matsushima, H. Odashima, D. Wang, S. Tsunekawa, K. Takagi, *Jpn. J. Appl. Phys. Part I* 33 (1994) 315.
- [20] H. Odashima, F. Matsushima, A. Kozato, S. Tsunekawa, K. Takagi, H. Linnartz, *J. Mol. Spectrosc.* 190 (1998) 107–111.
- [21] H. Odashima, A. Kozato, F. Matsushima, S. Tsunekawa, K. Takagi, *J. Mol. Spectrosc.* 195 (1999) 356–359.
- [22] J.M. Brown, D.A. Jennings, M. Vanek, L.R. Zink, K.M. Evenson, *J. Mol. Spectrosc.* 128 (1988) 587.
- [23] P. Verhoeve, M. Versluis, J.J. Ter Meulen, W. Leo Meerts, A. Dymanus, *Chem. Phys. Lett.* 161 (1989) 195–201.
- [24] M. Radunsky, Ph.D. Thesis, University of California-Berkeley, 1989.